BACTERIAL MIXTURE IDENTIICATION USING RAMAN AND SURFACE-ENHANCED RAMAN CHEMICAL IMAGING

Jason Guicheteau*, Steven Christesen, Darren Emge
U.S. Army Edgewood Chemical Biological Center Aberdeen Proving Ground, MD, USA 21010-5424
Ashish Tripathi, Rabih Jabbour
Science Applications International Corporation, Gunpowder Branch, Aberdeen Proving Ground, MD 21010-0068

ABSTRACT

A number of recent studies by this group and others have demonstrated the ability of normal Raman and surface-enhanced Raman spectroscopy (SERS) to identify bacteria at the species level. Our efforts have focused on the use of colloidal silver as the SERS active substrate. The addition of silver nanoparticles to the bacteria not only produces an enhanced Raman signal, but it also suppresses the native biofluorescence associated with visible laser excitation. Raman chemical imaging uses every pixel or a binned pixel group of the Raman camera as an independent Raman spectrograph. Thus, spatially resolved Raman spectral information is obtained; much like a visual microscope provides spatially resolved visual information. The advantage of this technique in biological detection resides primarily in analysis of biological samples in complex backgrounds without the need for any sample pre-processing. Using a chemical imaging Raman microscope, we compare normal Raman chemical imaging to SERS chemical imaging of a complex mixture of bacteria. In both cases we are able to differentiate single bacteria in the Raman microscope's field of view, but with a substantial reduction in analysis time for SERS chemical imaging.

1. INTRODUCTION

The chemical imaging component of Raman spectroscpoy has matured at a relatively rapid pace since its introduction approximately a decade ago. With respect to sample preparation and handling, Raman chemical imaging microspectroscopy (RCIM) is reagentless, remarkably simple, and straightforward. The relative purity of a substance can be obtained, and the individual components and structural details of a complex sample can be visualized in a noninvasive manner. A multivariate analysis translation of the Raman spectra provides a chemical or biochemical interpretation of the sample. An overlay of the bright field image (BFI) under the microscope and the Raman physical-to-chemical spectroscopic translation map produces a visual, colored analysis with inorganic/organic functional group, species, and component interpretation for the entire field of view (FOV).

RCIM analysis has been adapted to a wide variety of substance characterization investigations across a broad spectrum of industries, including automotive[1-,3], particulate matter characterization[4], pharmaceutical[5-7], and medical[9-24] .Furthermore, two recent reports show the feasibility of applying RCIM for the visualization of bacteria on a microscope slide[25,26].
This work focuses on comparing RCIM to surface-enhanced Raman chemical imaging microscopy (SERCIM) for the identification and detection of bacterial cells both isolated and in the presence of a complex mixture. Initially, vegetative cells of *Bacillus thuringiensis* are compared between the two techniques, followed by a mixture comparison of *Bacillus anthracis sterne* spores (BASP) and vegetative cells of *Bacillus cereus* (BCVG)

1.2 Raman Chemical Imaging Analysis

Raman Chemical Imaging allows for isolating a single Raman spectrum being scattered from a single bacterial cell. This isolation provides the advantage of analyzing samples which may contain impurities or even a complex mixture of various bacterial cells. The Raman chemical imaging converts pixels or binned groups of pixels of a CCD detector into isolated Raman spectra. A liquid crystal tunable filter (LCTF) provides the wavelength tenability for generating Raman spectra. At each tuned wavelength a Raman Image is acquired by exposing the pixels of the CCD detector to the scattered radiation. Thus a sequence of Raman images is acquired constituting a Raman Hyper Spectral Cube (RHSC). Figure 1 shows a visual representation of this process. In the experiments reported in this study the pixels are binned in 3x3 groups to improve the signal to noise ratio. The LCTF was programmed to scan the fingerprint region from 500 to 1850 cm^{-1} wavenumbers with a 10 cm^{-1} bandwidth. Thus, each RHSC comprised 136 image frames. The post acquisition processing and analysis of the RHSC was done with ChemImage Xpert 2.0 (ChemImage, Pittsburgh, USA). Cosmic and binary filtration were applied to all the acquired RHSCs. To perform the binary filtration, all the images frames in the RHSC were added. The summed image was binarized, by equating all the pixels intensities below a threshold to zero and above the threshold to one. All the image frames in the processed RHSC were multiplied by the binarized

Report Documentation Page

Form Approved
OMB No. 0704-0188

1. REPORT DATE	2. REPORT TYPE	3. DATES COVERED
DEC 2008	**N/A**	**-**

4. TITLE AND SUBTITLE	5a. CONTRACT NUMBER
Bacterial Mixture Identiication Using Raman And Surface-Enhanced Raman Chemical Imaging	5b. GRANT NUMBER
	5c. PROGRAM ELEMENT NUMBER
6. AUTHOR(S)	5d. PROJECT NUMBER
	5e. TASK NUMBER
	5f. WORK UNIT NUMBER
7. PERFORMING ORGANIZATION NAME(S) AND ADDRESS(ES) **U.S. Army Edgewood Chemical Biological Center Aberdeen Proving Ground, MD, USA 21010-5424**	8. PERFORMING ORGANIZATION REPORT NUMBER
9. SPONSORING/MONITORING AGENCY NAME(S) AND ADDRESS(ES)	10. SPONSOR/MONITOR'S ACRONYM(S)
	11. SPONSOR/MONITOR'S REPORT NUMBER(S)

12. DISTRIBUTION/AVAILABILITY STATEMENT
Approved for public release, distribution unlimited

13. SUPPLEMENTARY NOTES
See also ADM002187. Proceedings of the Army Science Conference (26th) Held in Orlando, Florida on 1-4 December 2008, The original document contains color images.

14. ABSTRACT

15. SUBJECT TERMS

16. SECURITY CLASSIFICATION OF:			17. LIMITATION OF ABSTRACT	18. NUMBER OF PAGES	19a. NAME OF RESPONSIBLE PERSON
a. REPORT	b. ABSTRACT	c. THIS PAGE			
unclassified	**unclassified**	**unclassified**	**UU**	**6**	

Standard Form 298 (Rev. 8-98)
Prescribed by ANSI Std Z39-18

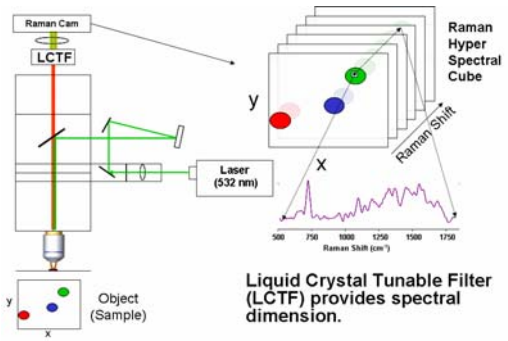

Figure 1. LCTF based Raman Chemical Imaging

image frame. Thus, the intensities of those binned pixel groups which were not exposed to Raman active sample were zeroed, while the intensities of binned pixel groups exposed to Raman active sample were retained. Principal component analysis (PCA) was performed on the resultant RHSC. Spectra extracted from each binned pixel group were treated as a case (Raman spectrum), and each frame or wavenumber was treated as a dimension in multivariate dataspace. The information in the first 15 principal components was used, as they represented 99.5% of the dataset variance. Selected principal component projections were assigned colors and the resulting color image was superimposed on the bright-field image of the sample.

2. EXPERIMENTAL

2.1 Silver Colloid Preparation

Silver nanoparticle suspensions were prepared following a modified procedure of Lee and Meisel[27]. In a one-liter three neck round bottom flask, 90 mg of silver nitrate (99+ %, Aldrich) were dissolved in 400 mL of deionized water (18.3 MΩ). In order to control volume loss due to evaporation a condenser (250 mm jacket length) was placed on the center neck of the flask. A 25 mL addition funnel with 10 mL of a 1% aqueous sodium citrate solution was attached to a second neck of the flask. A heating mantle was controlled by a 140-volt power-stat to bring the silver nitrate solution to a controlled boil in approximately 24 minutes. A one inch stir bar was placed in the reaction flask and set to stir at a rapid pace. In addition to the heating mantle, a heating top was placed around the flask to maintain temperature stability. Upon boiling, sodium citrate was added rapidly (stop cock fully opened). Heating and stirring were maintained for 45 minutes after addition of citrate, at which time the reaction flask was removed from heat and allowed to cool to room temperature (with stirring continued). The resulting nanoparticle suspensions appeared yellowish-brown with an electronic absorption λ_{max} of 400 nm and an average full width half maximum of 65 nm with an average particle size of 36 nm.

2.2 Bacteria

Aqueous suspensions of *Bacillus thuringiensis* vegetative cells and spores, *Bacillus anthracis sterne* spores (BASP) and vegetative cells of *Bacillus cereus* (BCVG) ATCC #11778 were supplied by the ECBC Biodefense. Samples were diluted using 18.3 MΩ H_2O to approximately 0.1 mg/mL

2.3 Microscope Slide Preparation

For normal Raman spectroscopic studies, a 5-µL aliquot of the sample was spotted from aqueous suspension on an aluminum coated microscope slide (ChemImage, Pittsburgh, USA) and allowed to dry in a bio-safety hood. SERS samples were prepared by, mixing a 3-µL aliquot of silver colloids with a 2-µL aliquot of the bacterial sample. The mixture was deposited on an Al-microscope slide and allowed to dry. Figure 2 shows spore of *Bacillus anthracis sterne* coated with silver nanoparticles. The FOV for all experiments were chosen in the near central regions of the dried spot. The edge of a spot experienced bacteria aggregation while the central regions of a spot displayed a dispersion of bacteria.

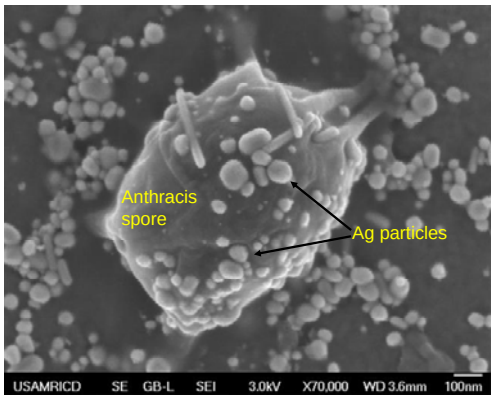

Figure 2. Bacillus anthracis spore coated with silver nanoparticles

2.4 Raman Instrumentation

The Raman chemical images were collected with a Raman Chemical Imaging Microscope (FALCON II, ChemImage, Pittsburgh, PA) equipped with a 532 nm laser excitation source and a 50x magnification objective. In order to reduce fluorescence from the biolgocial material all normal Raman samples were photobleached for at least 5 minutes prior to spectral acquisition and spectra were obtained using a constant laser power of 50 mW was set. For SERS analysis the laser power was reduced to 10 mW. Raman spectra were obtained in the 400-4100 cm^{-1} wavenumber region with a resolution of 3

cm^{-1}. Raman images were collected between 500 to 1850 cm^{-1} with 10 cm^{-1} resolution.

3. RESULTS AND DISCUSSION

3.1 Normal Raman Chemical Imaging of Bacillus thuringeinsis vegetative cells

A Sample of *B. thuringeinsis* vegetative cells (BTVG) was used to demonstrate the feasibility of extracting Raman spectra from a single bacterial cell. Normal Raman spectral analysis was performed with 60 seconds integration time per frame. Thus the 136 image frame RHSC was acquired in two hours and 16 minutes. Figure 3(a) shows the BFI of the BTVG cells present in the FOV. Average cell size was about 2.5 x 1.0 microns long. The RHSC was analyzed with the procedure outlined earlier. PCA was performed on the processed RHSC. The loading plot of principal component (PC) number two shows peaks at 1340,1370, and 1590 cm^{-1} wavenumbers. These bands are prominent features of the normal Raman spectra of BTVG, as shown in the library

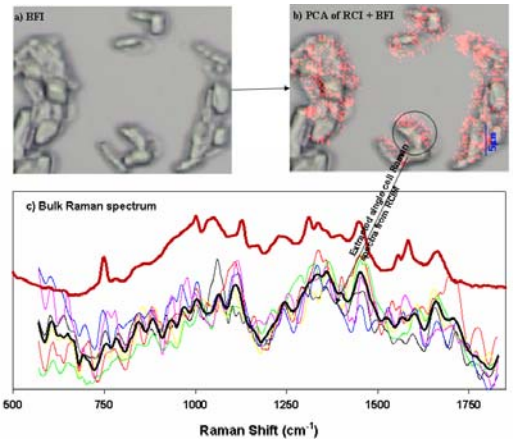

Figure 3. Normal Raman**.** RCI analysis of BTVG (a) BFI of BTVG; (b) Superimposition of PC # 4 projections (red) on BFI; (c) extracted Raman spectra from single cell (thin colored lines), avg. spectra (thick black line) library spectra of BTVG (thick red line).

spectra (Figure 3c, thick red line). The, 90 % or greater intensity projections of PC 2 were colored red and superimposed on the BFI image of BTVG (Figure 3b). Clearly, red regions are seen to be colocated with BTVG cells. However, the pixilated quality of various red regions is indicative of poor signal to noise (S/N) ratio of spectra recorded by the binned pixel group (BPG). One 3x3 BPG covers a 0.33 x 0.33 micron squared shaped area in the microscope FOV, and this is equivalent to an area of coverage of 0.11 square microns. Considering that a BTVG has an exposed surface area of two squared microns, each BPG records the spectra of only 5 % of a cell. Thus, S/N ratio is expected to be poor. Figure 3c shows the extracted Raman spectra from various cells (thin colored lines). The average of the six single cell extracted spectra is shown by thick black line in the Figure 3c. The S/N of the average spectra was evaluated by dividing the spectral intensity range (difference of maximum and minimum intensities) by the standard deviation of the spectral baseline. Thus for the average spectra, the S/N was estimated to be 26. Increasing the laser power density from 533 W/cm^2 may improve the signal intensities and minimize the noise, but it also increases the probability of photo damage to the cell. Another option to improve S/N is to increase the integration time from current value of 60 seconds per frame. However, that will increase the acquisition time from current duration of over two hours. A third option is to use SERS assisted RCI.

3.2 SERS assisted Raman Chemical Imaging of Bacillus thuringiensis vegetative cells

BTVG cells coated with silver nanoparticles were analyzed with RCIM. To obtain the RHSC, the integration time was set at 1 second per image frame. Thus the acquisition time to obtain the 136 image frame RHSC was 2 minutes and 16 seconds. Figure 4(a) shows the BFI of the nanoparticle coated BTVG cells present in the FOV. Due to the attachment of silver nanoparticles to the exteriror of the bacterial cells, the cells appear darker than the BTVG cells in figure 3a. The RHSC was analyzed with the procedure outlined above and a PCA was again performed on the processed RHSC. PC number five was selected to represent BTVG cells. The rationale for selection of PC number five is that the loading plot of this PC shows peaks at 730, 1060, 1340 and 1590 cm^{-1} wavenumbers. These bands are prominent features of the SERS Raman spectra of BTVG, as shown in the library

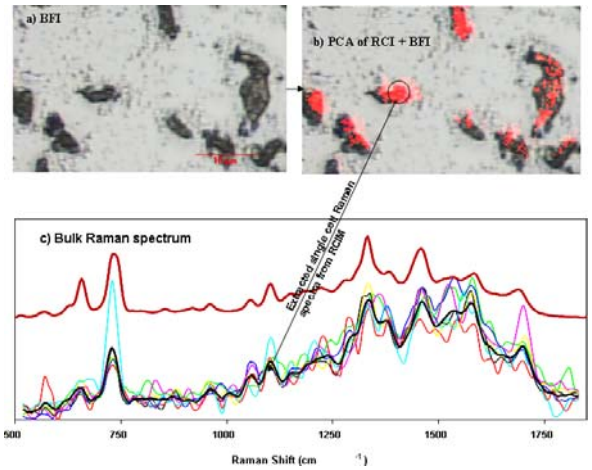

Figure 4. SERS. RCI analysis of BTVG (a) BFI of BTVG; (b) Superimposition of PC # 4 projections (red) on BFI; (c) extracted Raman spectra from single cell (thin colored lines), avg. spectra (thick black line) library spectra of BTVG (thick red line).

spectrum in figure 4c (thick red line). Thus, 80 % or greater intensity projections of PC 5 were colored red and superimposed on the BFI image (Figure 4b). Clearly, red regions are seen in co-location with BTVG cells. Visual examination of the pixel density of red regions shows denser clustering for SERS-BTVG cells when compared to normal BTVG cells (Figure 3b). This is indicative of better signal to noise (S/N) ratio of spectra recorded by the BPG's. Figure 4c shows the extracted Raman spectra from various cells (thin colored lines) and the average of the six single spectra (thick black line). The S/N of the average spectra was estimated to be 226. This is a factor of ten times improvement in the S/N when compared with the normal Raman sample. Furthermore, the acquisition time of two minutes and 16 seconds for SERS-BTVG is sixty times quicker than the two hours and 16 minutes acquisition time for normal-BTVG samples. Also the energy density used for this SERS experiment was 92 W/cm^2, which is six times less than the energy density of 533 W/cm^2 used for the normal Raman experiments. Combining these parameters of improved S/N, reduced acquisition time and laser energy density, the SERS is estimated to achieve factor of 3000 enhancement over the normal Raman

3.3 SERS assisted Raman Chemical Imaging of a bacterial mixture

In order to further show the utility of RCIM we prepared a slide containing a mixture of *Bacillus anthracis sterne* spores (BASP) and vegetative cells of *Bacillus cereus* (BCVG). The data presented below only concerns SERS assisted RCIM, however a normal Raman slide was generated and analyzed as well, and will be compared at the end. The RHSC was obtained with a set integration time of 0.5 seconds per image frame with four co-adds. Thus, the 136 image frame RHSC was acquired in four minutes and 32 seconds. Figure 5 shows the process used in the constrction of the RGB image derived from the PCA analysis of the RHSC. First, the two PC's which carry the partial features of the two bacteria were identified. PC 9 was found to represent BCVG, thus 90 % or greater projection values of PC 9 were colored green (Figure 5a). Similarly, PC 10 was found to represent BASP and 90 % or greater projection values of PC 10 were colored red (Figure 5b). The two images were combined resulting in the RGB image (Figure 5c). Figure 5d shows the BFI of the mixture of the two bacteria. The rod shaped bacteria are the BCVG, while oval shaped bacteria are the BASP. The RGB and BFI images were overlaid resulting in the image shown in Figure 5e. Clearly, mostly green regions correspond with BCVG, while the red regions correspond with BASP. The Figure 6b shows the extracted Raman spectra (thin colored lines) from single BA spores (red regions in the Figure 6a), along with the library spectrum of BASP (thick red line).

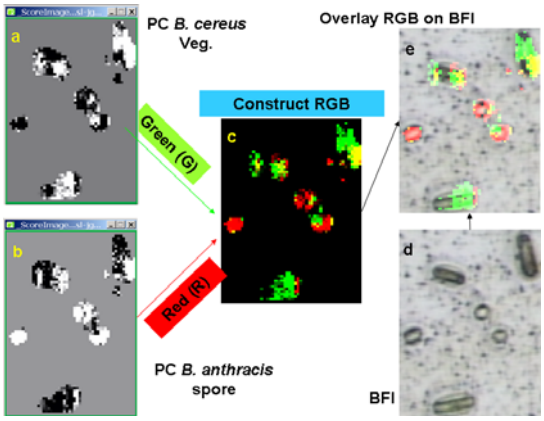

Figure 5. Construction of the RGB image from the PCA analysis of bacterial mixture RHSC.

Visually, the extracted spectra from single spores match with the library spectra. The S/N of the average of the three single spore spectra (black line) is estimated to be 112. The Figure 6c shows the extracted Raman spectra (thin colored lines) from single BC vegetative cells (green regions in the Figure 6a), along with the library spectrum of BCVG (think red line). The extracted spectra from single cells match, visually, with the library spectra. The S/N of the average of the three single cell spectra (black line) is estimated to be 242. The primary reason that S/N of BCVG is twice as large as that of BASP is because the BCVG cells are twice the size of BASP. Thus, the number of BPGs exposed to each cell is twice the number of BPGs exposed to each spore.

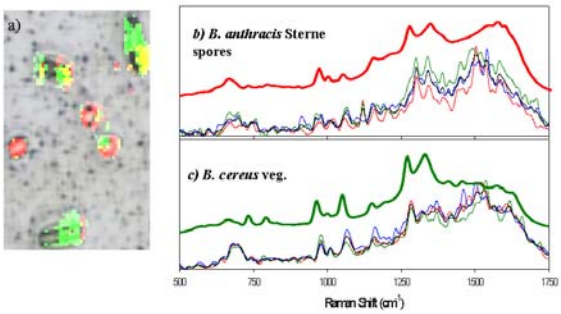

Figure 6. SERS (a) Processed RGB image overlaid on BFI; (b) extracted Raman spectra from single spores (thin colored lines), avg. spectra (black line) library spectra of BASP(thick red line). (c) extracted Raman spectra from single cells (thin colored lines), avg. sp(black line) library spectra of BCVG(thick red line).

The extracted SERS spectra from single BTVG (Figure 4c), BASP (Figure 6b) and BCVG (Figure 6c) were analyzed using PCA. Figure 7 shows a plot of PC 1, 2 and 3 projections. The three PC projections of the spectra from each of the three bacterial tend to form clusters with minimal overlaps between clusters. Clearly,

the S/N of single organism spectra is sufficient to allow for discrimination between these BCVG (blue triangles), BASP (green circles) and BTVG (red squares) organisms.

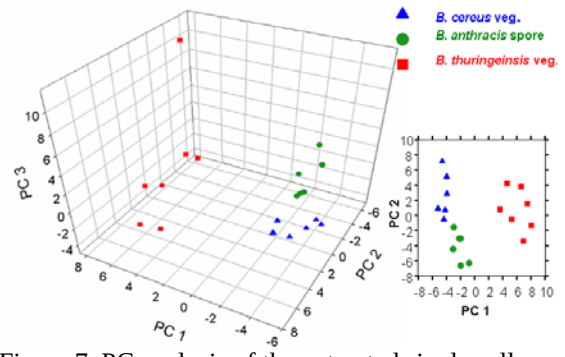

Figure 7. PC analysis of the extracted single cell spectra.

As mentioned above a BASP-BCVG was prepared and analyzed without nanoparticle attachment. The data did show distinguahsble peaks comparable to the SERS data. However, with the estimated power density delivered at the FOV to be 1511 W/cm^2, a decrease of S/N to 60 and a total analysis time being four hours and 32 minutes the an ehnacement factor for the SERS data was estimated to be 5000 and 3700 over the normal Raman for BASP and BCVG respectively.

4. CONCLUSIONS

Raman chemical imaging microscopy allows for extraction of spectra emanating from single bacterial cells and spores. Consequently, RCIM allows for detection of a mixture of bacteria present in the same FOV. The spectral quality of non-SERS bacterial sample was less than that of the SERS; while the acquisition time of the RHSC was several hours long. The attachment of silver nano-particles to the bacterial samples not only improved the S/N but also substantially reduced the acquisition time. SERS was estimated to enhance the Raman spectra by a factor of three to five thousand.

ACKNOWLEDGEMENTS

The authors of this paper thank Laurie Fazekas Carey and Catherine Rodriques of the Biodefense Branch at ECBC for supplying the bacterial samples investigated in this paper. We also thank Tracey Hamilton at the US Army Medical Research Institute of Chemical Defense in assisting with acquisition of SEM data.

REFERENCES

1. Morris, H. R.; Munroe, B.; Ryntz, R. A.; Treado, P. J. *Langmuir* 1998, **14**, 2426-2434.
2. Morris, H. R.; Turner II, J. F.; Munro, B.; Ryntz, R. A.; Treado, P. J. *Langmuir* 1999, **15**, 2961-2972.
3. Stellman, C. M.; Booksh, K. S.; Myrick, M. L. *Appl. Spectrosc*. 1996, **50**, 552-557.
4. Nelson, M. P.; Zugates, C. T.; Treado, P. J.; Casuccio, G. S.; Exline, D. L.; Schlaegle, S. F. *Aerosol Sci. Technol. 2001*, ***34,*** 108-117.
5. Nishikida, K; Lowry, S. *Suppl. Spectrosc.* 2006, June, 44-50.
6. Slobodan, S.; Clark, D. A. *Appl. Spectrosc.* 2006, **60**, 494-502.
7. Lin, W.-Q.; Jiang, J.-H.; Yang, H.-F.; Ozaki, Y.; Shen, G.-L.; Yu, R.-Q. *Anal. Chem.* 2006, **78**, 6003-6011.
8. Timlin, J.A.; Carden, A.; Morris, M. D.; Rajachar, R. M.; Kohn, D. H. *Anal. Chem.* 2000, **72**, 2229-2236.
9. Timlin, J. A.; Carden, A.; Morris, M. D.; Bonadio, J. F.; Hoffler II, C. E.; Kozloff, K. M.; Goldstein, S. A. *J. Biomed. Optics* 1999, **4**, 28-34.
10. Kline, N. J.; Treado, P. J. *J. Raman Spectrosc.* 1997, **28**, 119-124.
11. Nijssen, A.; Bakker Schut, T. C.; Heule, F.; Caspers, P. J.; Hayes, D. P.; Neumann, M. H.; Puppels, G. J. *J. Invest. Dermatol.* 2002, **119**, 64-69.
12. Shafer-Peltier, K. E.; Haka, A. S.; Motz, J. T.; Fitzmaurice, M.; Dasari, R. R.; Feld, M. S. *J. Cellular Biochem. Suppl.* 2002, **39**, 125-137.
13. van der Poll, S. W. E.; Bakker Schut, T. C.; van der Laarse, A.; Puppels, G. J. *J. Raman Spectrosc.* 2002, **33**, 544-551.
14. Shafer-Peltier, K. E.; Haka, A. S.; Fitzmaurice, M.; Crowe, J.; Myles, J.; Dasari, R. R.; Feld, M. S. *J. Raman Spectrosc*. 2002, **33**, 552-563.
15. Kniepp, J.; Bakker Schut, T.; Kliffen, M.; Menke-Pluijmers, M.; Puppels, G. *Vib. Spectrosc.* 2003, **32**, 67-74.
16. Smith, J.; Kendall, C.; Sammon, A.; Christie-Brown, J.; Stone, N. *Technol. Cancer Res. Treatment* 2003, **2**, 327-331.
17. Eliasson, C.; Engelbrektsson, J.; Loren, A.; Abrahamsson, J.; Abrahamsson, K.; Josefson, M. *Chemom. Intell. Lab. Syst.* 2006, **81**, 13-20.
18. Krafft, C.; Knetschke, T.; Funk, R. H. W.; Salzer, R. *Anal. Chem*. 2006, **78**, 4424-4429.
19. de Jong, B. W. D.; Bakker Schut, T. C.; Maquelin, K.; van der Kwast, T.; Bangma, C. H.; Kok, D.-J.; Puppels, G. J. *Anal. Chem*. 2006, **78**, 7761-7769.
20. Taleb, A.; Diamond, J.; McGarvey, J. J.; Beattie, J. R.; Toland, C.; Hamilton, P. W. *J. Phys. Chem. B* 2006, **110**, 19625-19631.
21. Koljenovic, S.; Choo-Smith, L.-P.; Bakker Schut, T. C.; Kros, J. M.; van der Berge, H. J.; Puppels, G. J. Lab. Invest. 2002, **82**, 1265-1277.
22. Koljenovic, S.; Bakker Schut, T.; Vincent, A.; Kros, J. M.; Puppels, G. J. *Anal. Chem.* 2005, **77**, 7958-7965.
23. Matthaus, C.; Boydston-White, S.; Miljkovic, M.; Romeo, M.; Diem, M. *Appl. Spectrosc.* 2006, **60**, 1-8.

24. Koljenovic, S.; Bakker Schut, T. C.; Wolthuis, R.; Vincent, A. J. P. E.; Hendriks-Hagevi, G.; Santos, L.; Kros, J. M.; Puppels, G. J. *Anal. Chem.* 2007, **79**, 557-564.
25. Kalasinsky, K. S.; Hadfield, T.; Shea, A. A.; Kalasinsky, V.; Nelson, M. P.; Neiss, J.; Draush, A. J.; Vanni, G. S.; Treado, P. J. *Anal. Chem.* 2007, **79**, 2658-2673.
26. A. Tripathi, R. E. Jabbour, P. J. Treado, J. H. Neiss, M. P. Nelson, J. L. Jensen, and A. P. Snyder, Appl. Spectrosc. Submitted (2007).
27. P.C. Lee and D. Meisel, J Phys Chem, 1982, **86,** 17, 3391-3395.